

# FLOW CONTROL ACTUATOR IN MICROCHANNEL

By

Shih-Chieh Chang

A Thesis Submitted to the Graduate

Faculty of Rensselaer Polytechnic Institute

in Fulfillment of the

Requirements for the Degree of

MASTER OF SCIENCE

Major Subject: MECHANICAL ENGINEERING

Approved:

---

Professor: Yoav Peles    Thesis Adviser

Rensselaer Polytechnic Institute  
Troy, New York  
April 2010  
(For Graduation May 2010)

© Copyright 2010

by

Shih-Chieh Chang

All Rights Reserved

# TABLE OF CONTENTS

TABLE OF CONTENTS .....	iii
LIST OF FIGURES .....	iv
ACKNOWLEDGEMENT .....	v
ABSTRACT .....	vi
1. INTRODUCTION	
1.1 Motivation .....	1
1.2 Organization and Scope of Thesis .....	3
2. EXPERIMENTAL SETUP & PROCEDURE	
2.1. Facility Setup	
(a) Main Working System .....	4
(b) Flow Control System .....	4
2.2. Experimental Procedure .....	8
3. RESULTS & DISCUSSION	
3.1. Droplets Issue Into Stagnation gas .....	9
3.2. Jet Issue Into Microchannel (Gas Main Flow) .....	17
4. CONCLUSIONS .....	25
REFERENCES .....	27

## LIST OF FIGURES

Figure 2-1 Experiment setup schematic plan -----	5
Figure 2-2 Bottom view of the micro device -----	6
Figure 2-3 Bottom view of the micro device packaging -----	6
Figure 2-4 Actuator 3D CAD profile -----	6
Figure 2-5 Actuator operating voltage profile -----	6
Figure 2-6 Controlling signal diagram -----	7
Figure 2-7 Optimum open time in logarithm of open time in millisecond -----	8
Figure 3-1 (a) - (f) OTE % for pressure dependent -----	10
Figure 3-2 (a) - (e) Pressure dependence for logarithm OTE% at specific logarithm controlled open time -----	13
Figure 3-3 (a) - (e) Actual frequency performance -----	15
Figure 3-4 (a) - (f) AFE % for pressure dependence -----	18
Figure 3- 5 (a) - (e) AFE% for duty cycle dependence -----	21
Figure 3- 6 Cross-section schematic diagram for the connecting zone -----	23
Figure 3-7 Illustration for the droplets in microchannel -----	24

## ACKNOWLEDGEMENT

I would like to present my great thanks to some very important people for this project. First, I really appreciate Professor Yoav Peles, my advisor, and Michael Amitay to giving me the precious opportunity join the Heat Transfer and Flow Control in Microsystems Research Group and work with them. Under Professor Peles and Amitay's guidance with their wisdom, patience, and great support, this work could be completed successfully. I truly cherish the learning experience with Professor Peles and Amitay. Secondly, I want to thank Daren Elcock, Farzad Houshmand, Junkyu Jung and Dr. Chih-Jung Kuo. In these two years of studying in R.P.I., we have worked, studied, chatted together, and I received many assistances from them; it let me learned not only just research experiences but also the different values of multiple cultures. Finally, of course, I have to present my greatest appreciation to my family with the enormous regards I have for them. Because of your endless love and support, I have the courage to take up any challenge. I will continue to work hard toward my dreams and hope one day I could help others as you have helped me.

## ABSTRACT

An experimental study of a flow control actuator has been conducted to obtain its basic characteristics and determine its performances in microchannel. Results showed that the error of the actual operating open time was increased while the controlled frequency was increased or the controlled duty cycle was decrease. The error of actual operating open time was not a function of pressure of the actuator. However, the performance of the actual operating frequency corresponded to the controlling signal.

The performance of the actuator in frequency was also robust ( $\pm 10\%$ ) when droplets were introduced into microchannel for every operating combinations. However, the actual operating frequency was always limited for lower duty cycle under lower working pressures. Similarly, higher duty cycle, which was 75 % in this study, also showed limitations in terms of operating frequency when working under lower pressure conditions of 5, 10, 25 Psi.

# I. INTRODUCTION

## 1.1 MOTIVATION

Owing to the progress of technology and the massive market of consumer electronic products, which have been advancing and improved continuously, not only the processing rate of the computational chips is increased but also the size of the products is reduced (thinner and narrower). The situation does not only happen for the consumer electronic products but also similarly occurs in the energy products such as the fuel cell module, LED packaging module, LCD monitor backlight, etc. Under the current designing trend, thermal management of electronic equipment can no longer be solved solely by using fins or with fans due to the reduced product size and the increased power density.

However, micro devices have high heat transfer performance because as the size of the channel decreases, the heat transfer coefficient increases [1]. The research about heat transfer in microchannel, regardless of single phase [2]–[6] or boiling [7]–[9], has been extensively studied and developed over the last decade in pursuit of better cooling method for high-powered electronic systems. Moreover, it has been shown that very high heat fluxes ( $790 \frac{W}{cm^2}$ ) can be dissipated with microchannel cooling. However, adopting flow control techniques in microchannel in order to increase flow mixing or reduce pressure drop was not widely developed in past studies.

After Prandtl(1904) brought forth the boundary layer theory, explaining the physical phenomena of separation and providing several experiment results about boundary layer control, the gate to the land of flow control research was opened, especially during the Second World War (1939-1945) and the subsequent Cold War (1945-1990).

Flow control can be classified into two categories: passive flow control and active flow control. Passive flow control is achieved through the use of bluff bodies to induce separation, vortex shedding, drag, and lift as discussed in a review study by Choi et al. [10]. In the realm of active flow control, two groups can also be found: open-loop and close-loop. Although close-loop control method possesses the advantages for accuracy and adjustable properties, it also has disadvantages. High cost and power demanded are the main shortcomings of close-loop feedback control, and creating a stable feedback law can also be a crucial challenge. In addition,

dynamical and accurate models can also be challenging because a model produced for flow regime may be invalid once feedback is introduced and dynamics of the flow is changed. Therefore, the collaboration between control designers, fluid dynamics, and modelers is demanded.

On the other hand, open-loop active flow control is attractive for its simplicity and generally requires less actuator power. Thus, this thesis focuses on open-loop. However, there are several approaches utilizing open-loop active flow control: steady mass injection, pulsed mass injection, zero net mass injection (synthetic jet), oscillating flap, piezoelectric device, etc.[11].

Hwang et al. [12] further conducted an experimental study to investigate the flow and heat transfer characteristics of an impinging jet controlled by vortex method of secondary shear flow and acoustic excitation. Enhancement or reduction in heat transfer in their experiment was obtained by changing the flow structure. In the experimental study of Inaoka et al. [13], miniature flapping actuator, which were mounted on the trail edge of a step, was utilized to alter the flow field and then repair the heat transfer deterioration due to the flow recirculation just behind the step though large heat transfer enhancement was achieved downstream the step.

However, the open-loop active flow control technique to manage the flow field in the microchannel is not much studied, but the applications of open-loop active flow control in conventional scale, using piezoelectric material diaphragm, flapper or speaker placed on specific location to generate the disturbances with the proper frequency and magnitude to control the separation so as to fulfill the demand, is prevalently applied in the industries especially in the aerospace industry. Nevertheless, the actuators of those applications on the macro scale, which are mounted on the control place might result in vibration of the entire micro device, so that the methods are not necessary appropriate for at the micro scale. Thus, considering the advantage of a valve, which can create miniature droplets that generate the liquid jet outside the microchannel before being introduced into the channel, a valve may be a suitable actuator and provides reasonable attempt to fulfill the task of flow control in a microchannel.

The purpose of thesis is to parametrically study a micro dispensing valve and its performance inside a microchannel.

## 1.2. ORGANIZATION AND SCOPE OF THESIS

The goal of the experimental study presented in this thesis is to provide comprehensive knowledge and data of the micro dispensing valve, which can be used as a flow control actuator. Chapter 2 describes the experimental facility setup and procedure. The results and discussion of the actuator's characteristics and performances in microchannel are presented in Chapter 3. The final chapter presents the summary and conclusion of the experimental study.

## II. EXPERIMENTAL SETUP & PROCEDURE

### 2.1 FACILITY SETUP

The concept of this application of flow control is to create disturbances in the microchannel by introducing miniature droplets via a micro dispensing valve. In this chapter, two systems (Main Working System & Flow Control System) will be described separately.

#### Main Working System

Figure 2-1 is a schematic plan of a experiment setup. For the main working system, in order to visualize the flow image, microscope is connected to a Vision Research Phantom V-4 series high-speed camera that is capable of capturing frames with a frame rate up to 90,000 per second, a highest resolution of 512 x 512 pixels and a minimum exposure time of 2 microsecond, and to a CCD camera with LAVISION Da Vis 7.2 Software for micro-particle image velocimetry ( $\mu$ PIV), which is necessary for monitoring the flow field and for further analysis.

The liquid reservoir, flow meter, filter, PCB piezoelectric pressure transducer, and microchannel packaging, are all located in sequential order on the working pipeline. The working fluid is pressurized from the reservoir through the entire pipeline. OMEGA FL-25766 flow meter is used for obtaining the flow rate. Due to the dimension of the micro-device that will be discussed in more details later, a filter rated for over 7 micro particles is installed upstream the microchannel. OMEGA PX303-100A5V piezoelectric pressure transducer monitored by LabVIEW detects the inlet pressure of the main working fluid.

The silicon device ( $w=10.2mm$ ,  $h=1.45mm$ ,  $\ell=32mm$ ) holds the microchannel ( $w=1500 \mu m$ ,  $h=205 \mu m$ ,  $\ell=27500 \mu m$ ), as shown in Figure 2-2. The micro-device is packaged into the working platform by sandwiching between two metals with miniature O-rings at each orifice on the device as shown in Figure 2-3.

#### Flow Control System

The creation of a stable, robust and functionable stream of droplets into the microchannel not only depends on the actuator, which will be introduced later, but also relies on the water reservoir, pressure regulator, filter, and PCB piezoelectric pressure transducer. Different from the

main working system, for flow control system, shown in Figure 2-1 (Flow control system line), the usage of the pressure regulator is needed to avoid exposing the entire system to high pressure (120 Psi), which would be harmful to the flow control actuator.

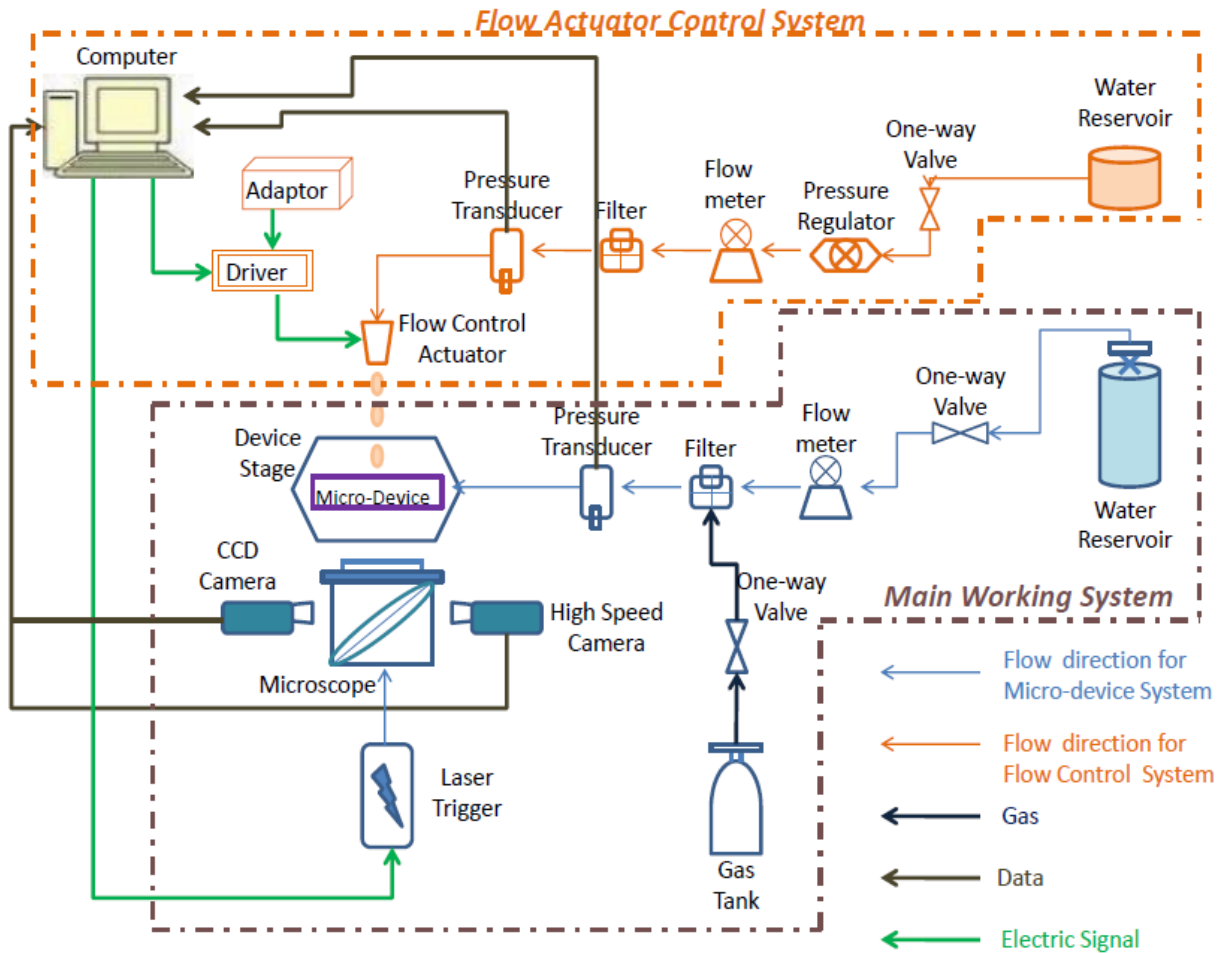


Figure 2-1 Experiment setup schematic plan

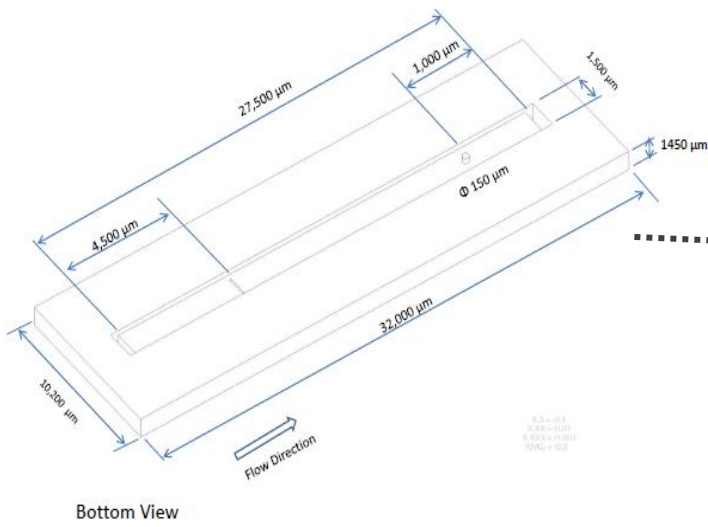


Figure 2-2 bottom view of the micro device

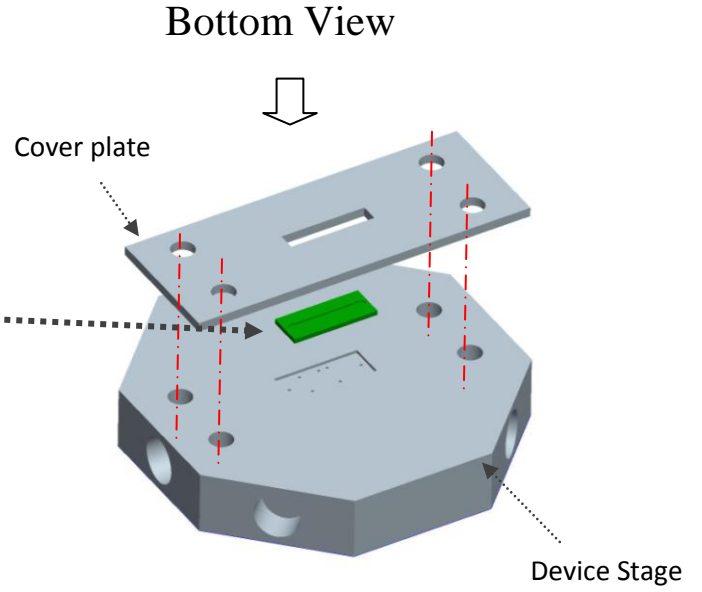


Figure 2-3 bottom view of the micro device packaging

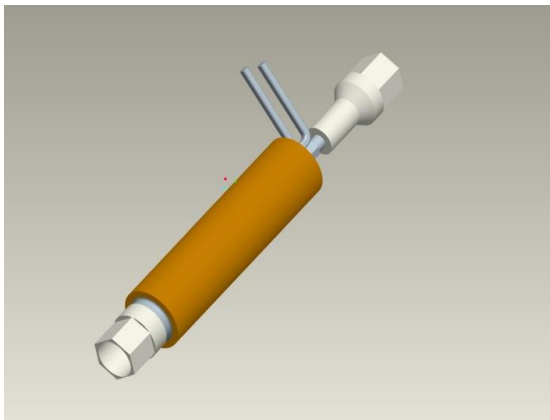


Figure 2-4 actuator CAD profile

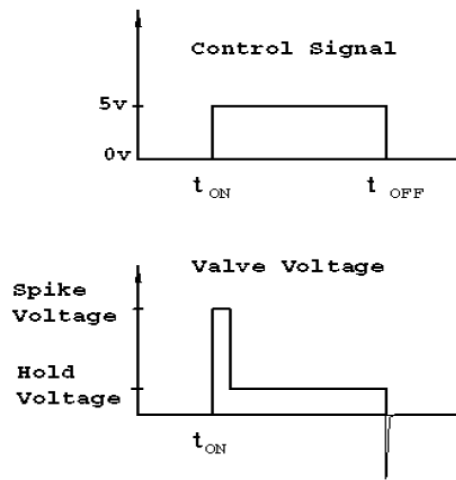


Figure 2-5 operating voltage profile

The actuator, made by LEE Company IKTX0322000AC micro-dispensing valve, provides the miniature droplets for the flow control, as shown in Figure 2-4. To maintain a proper functioning environment for the actuator, shown in Figure 2-5, 3.5V for the basic potential (Hold Voltage) is applied while 12V is supplied as the starting voltage (Spike Voltage). Both voltages are provided by the adaptors. In order to provide an adjustable 5V control signal (TTL), LabVIEW is programmed to manipulate the frequency and duty cycle of the droplets. Disturbances in the microchannel is obtained with a range of frequency between 0 and 1000 Hz and duty cycle from 1% to 100% ( Figure 2-6).

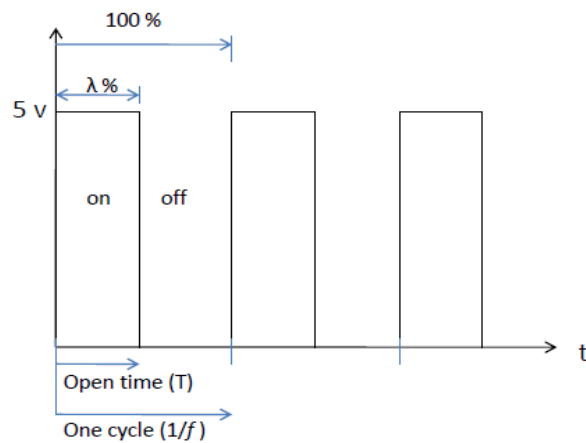


Figure 2-6 controlling signal diagram

As a result of changing frequency and duty cycle percentage, it alters the open time of the actuator — a critical parameter for the volume flow rate — so that the disturbances in the microchannel can be controlled. Theoretically, we can simply estimate the actuator open time via the following equation:

$$T = (1/f) \times (\lambda\%) \tag{1}$$

where  $f$  is the droplet frequency and  $\lambda$  represents the percentage duty cycle. Both  $f$  and  $\lambda$  are the controlled parameters.

Figure 2-7 shows the relationship between frequency and percentage of duty circle for the actuator open time of a single cycle. It is clear that there are two parameters for changing the single open time of the actuator — increasing frequency or reducing duty cycle percentage shorten the open time.

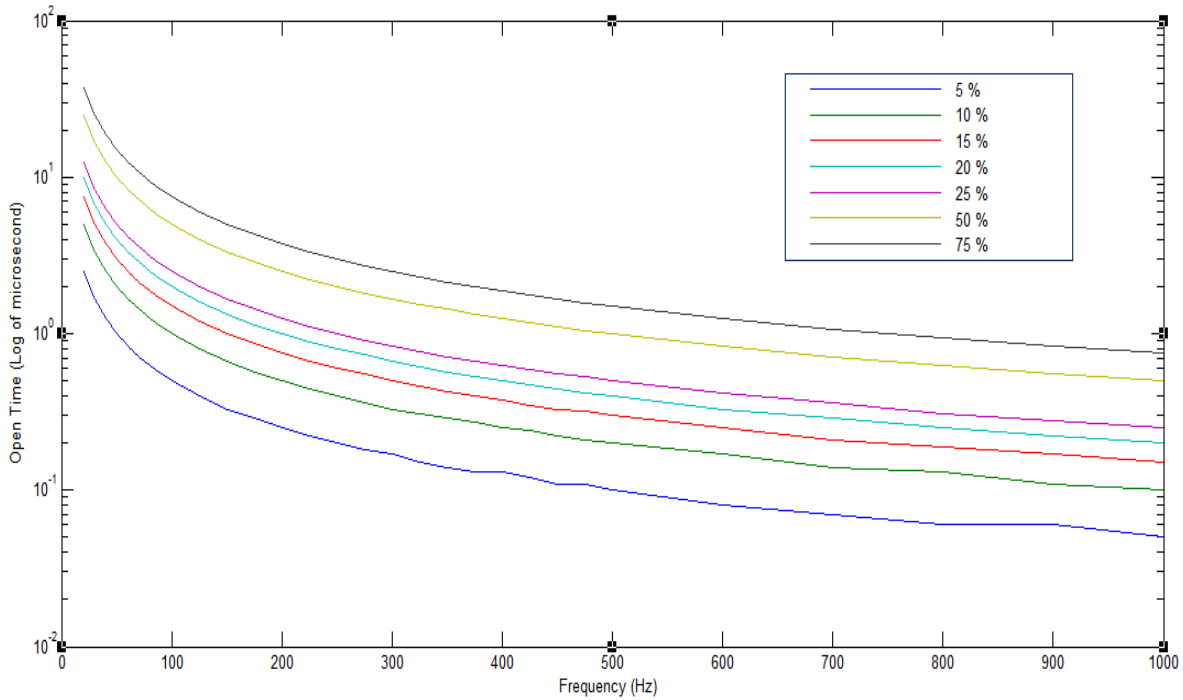


Figure 2-7 Optimum open time in logarithm of open time in millisecond

## 2.2 EXPERIMENTAL PROCEDURE

To confirm the actuator's characteristic and capability, pressure, frequency and duty cycle were examined in this experiment. In order to obtain the valuable data for further research, more experimental sets were demanded. The pressure was set to 5, 10, 25, 50, 75 and 100 Psi, and the duty cycle percentage was set at 5%, 10%, 25%, 50%, 75%. Furthermore, under each combination, the frequency was run at 5, 10, 25, 50, 75, 100 Hz, from 100 to 500 Hz with interval of 50 Hz and from 500 to 1000 Hz with interval of 100 Hz. The experimental data were quantified in charts presented in the next chapter.

### III. RESULTS AND DISCUSSION

#### (1) Droplets Issue Into Stagnation Gas

In this experiment, the purpose was to understand the basic characteristic of the actuator and to gain the database for further flow control research to calculate Reynolds Number, momentum ratio and Strouhal Number etc.,. However, for these non-dimensional numbers, the volume flow rate and the frequency of the controlled jet play critical roles. Therefore, the actual operating frequency of the actuator was examined. In addition, because the factor for the volume flow rate not only is depended on the pressure but also relies on the actuator's open time, the actual operating open time of the actuator was inspected

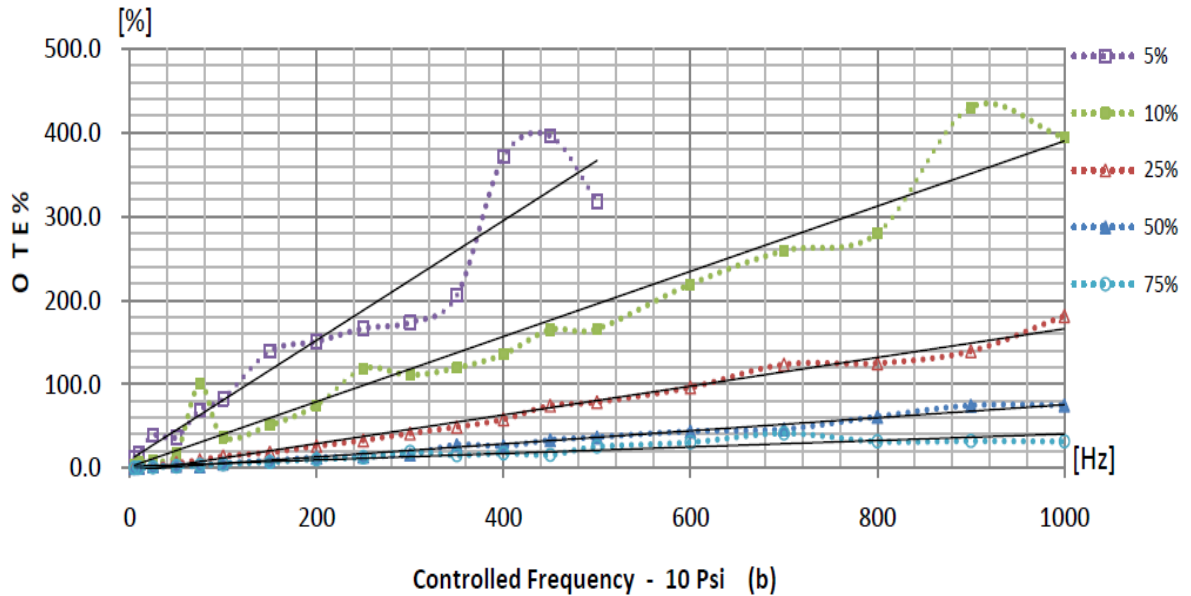
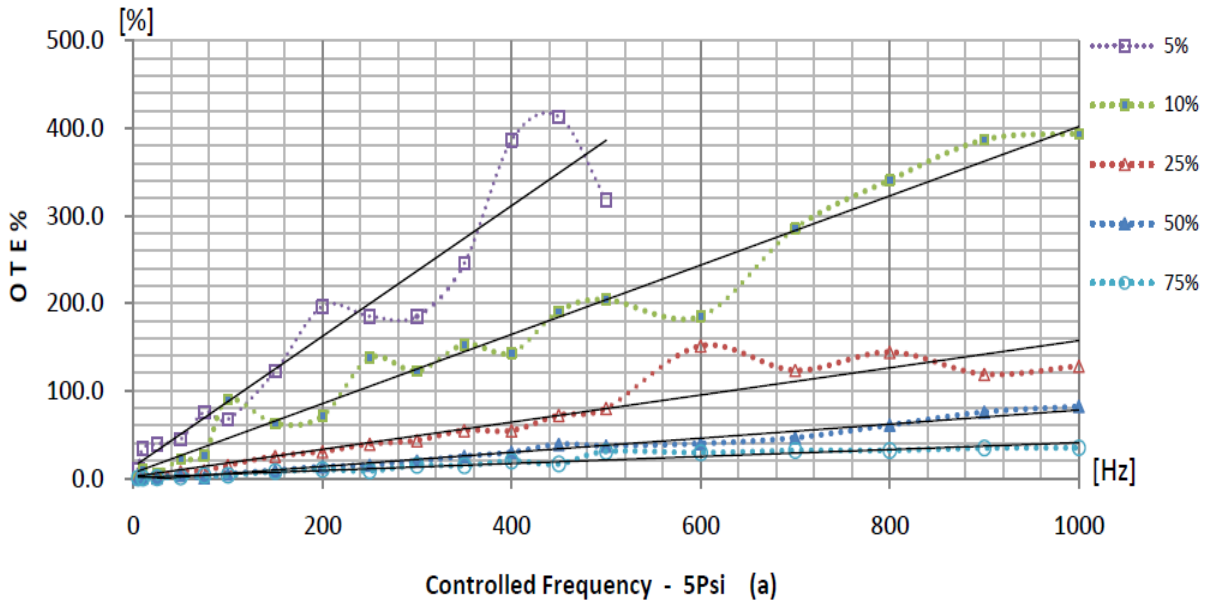
The experiment utilized a high speed camera with 53,000 frames per second with a time interval of 19 microseconds through a microscope to observe the droplet issuing into stagnation gas. From Figure 3-1 (a - f), the X-axis represents the frequency of the controlled signal, which was set on LabVIEW, and the Y-axis indicates the actual operating open time error percentage (OTE%) of the actuator, which was obtained from Equation (2):

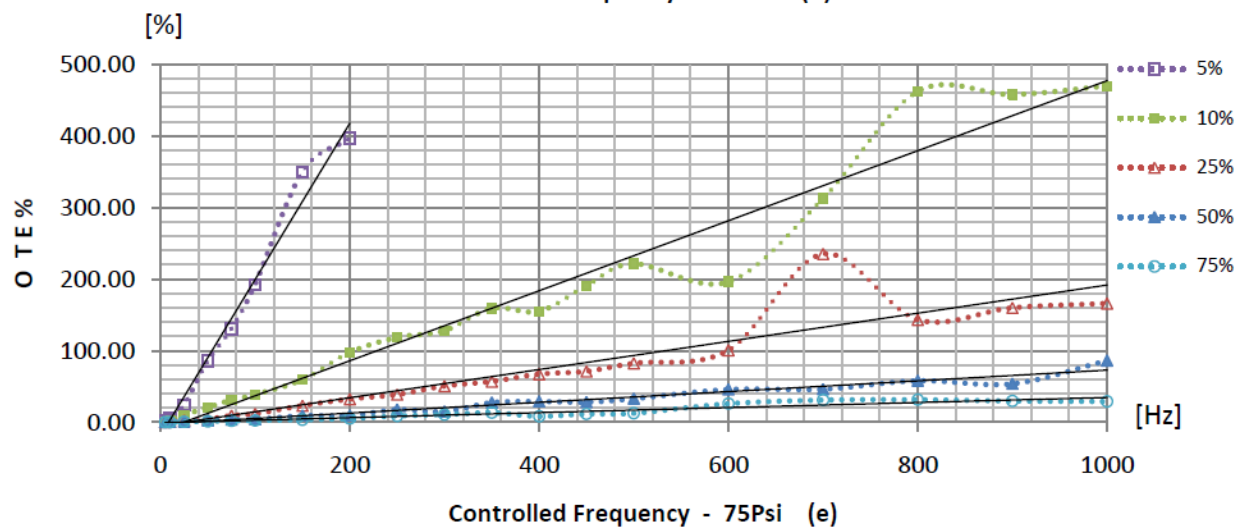
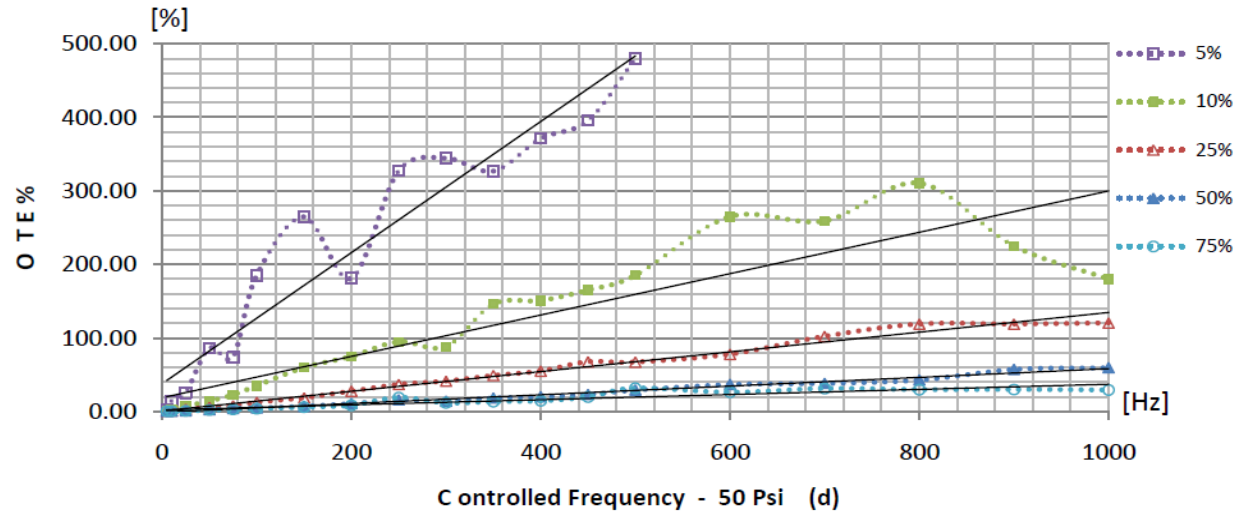
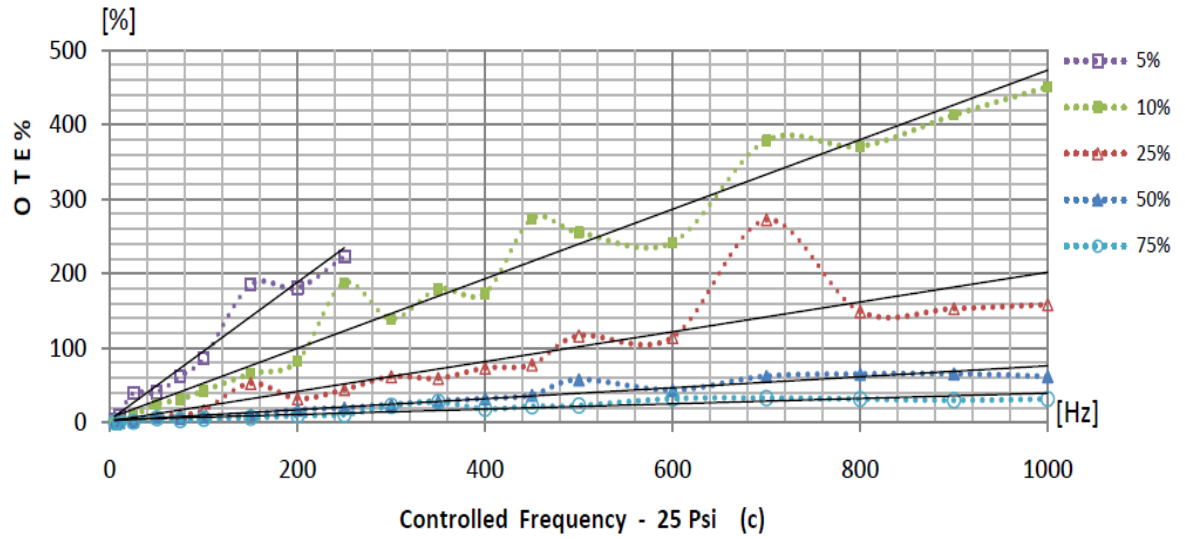
$$[OTE \%] = \left( \frac{R_o - C_o}{C_o} \right) \times 100 \% \quad (2)$$

where  $R_o$  is the actuator actual operating open time observed from the high speed camera, and  $C_o$  is the controlled open time set in LabVIEW.

As the data shown in the Figure 3-1 (a) to (f), it is clear that when the controlled frequency was increased under the same duty cycle percentage condition, the OTE% increased. Moreover, when the duty cycle percentage decreased the OTE% increased as well. Compared to the different pressures for the liquid reservoir on the flow control system, the actuator had similar trends of OTE%. When the controlled frequency increased with lower percentage duty cycle, the actuator operating open time was shortened, so that the OTE% increased. This was due to the on-off mechanism of the actuator been controlled by the coil to open and close the gate. That was the reason why when the controlled TTL signal was set at high frequency with low percentage duty cycle, the mechanical on-off motion of the actuator didn't accommodate such short open time. Therefore, actual open time error was considerable large. In addition, from Figure 3-1, the data of duty cycle of 5 % for the all pressures could not be generated after certain controlled

frequency. The reason is that small droplets were produced under a short operating open time and then the atomized droplets adhered around the nozzle to form a large water droplet preventing droplets from issuing into stagnation gas.





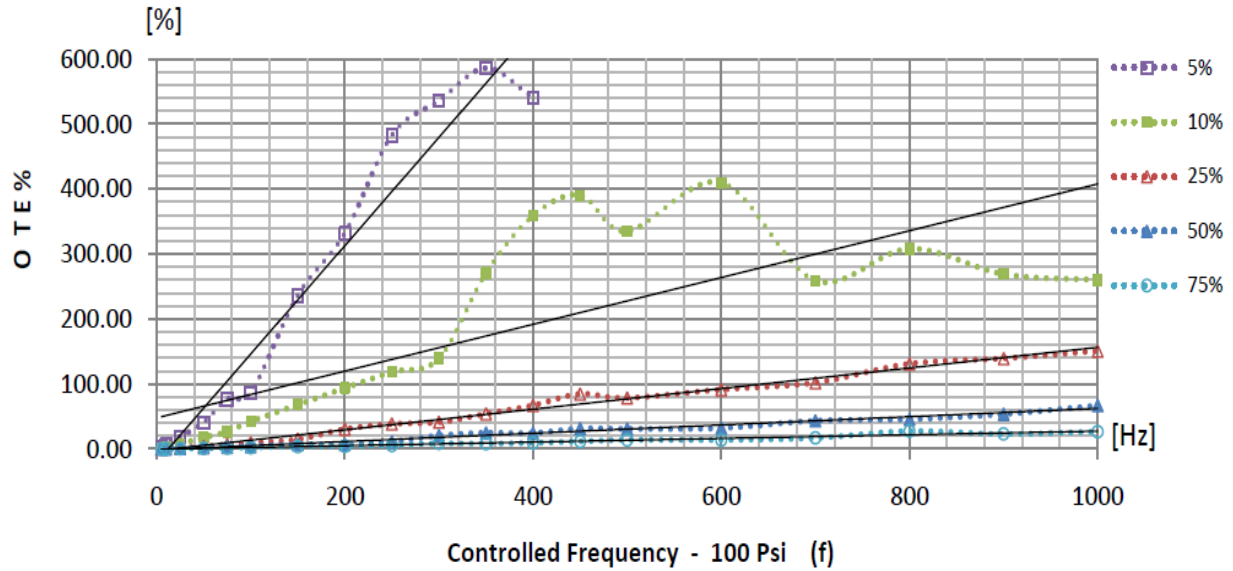
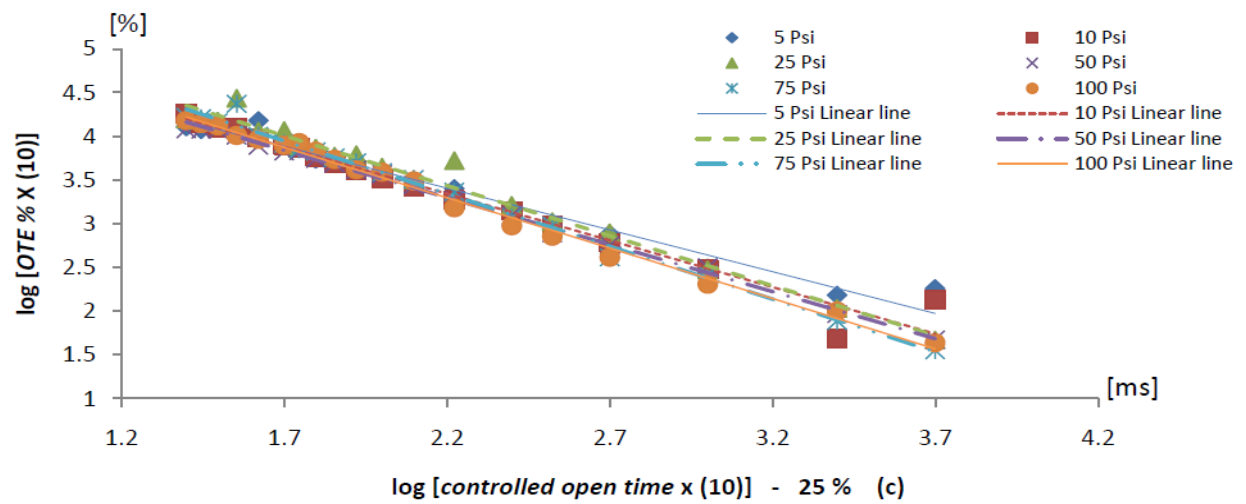
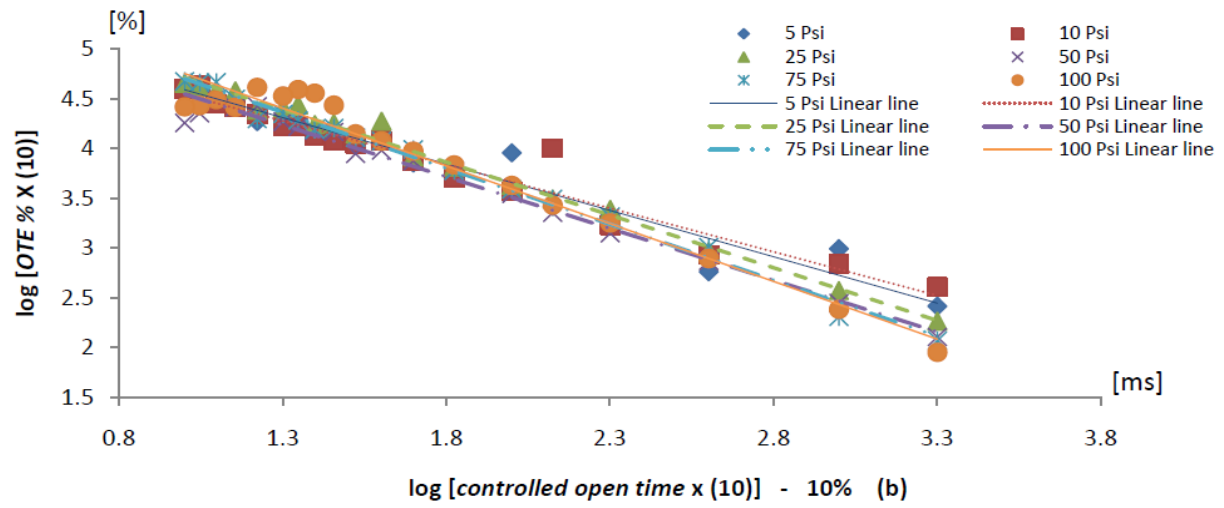
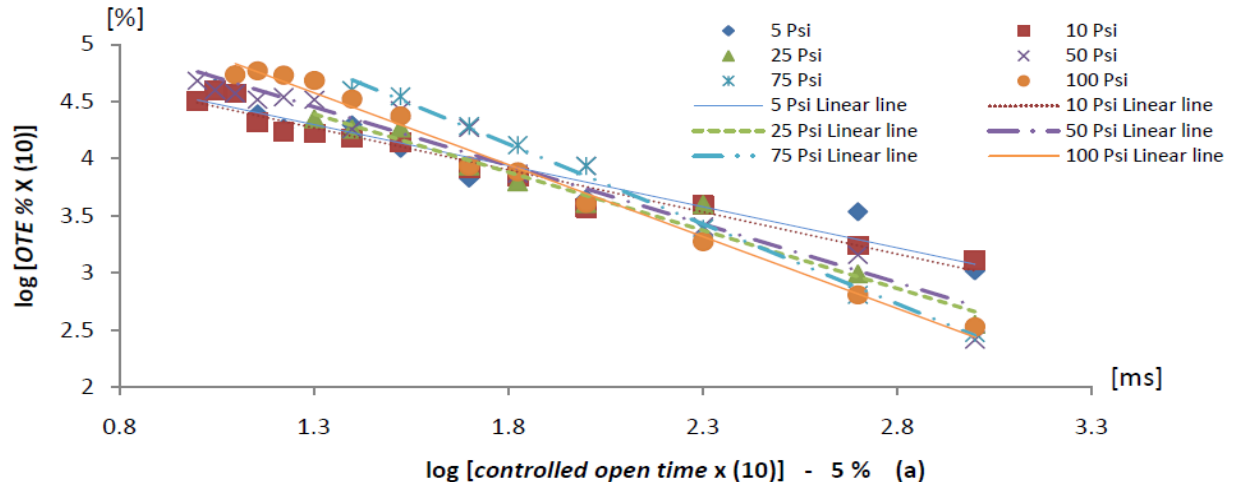


Figure 3-1 OTE % for pressure dependent

However, for these several experiment, different pressures for the actuator had the same controlled frequency and duty cycle percentage meaning the same open time. The role of different pressures for the OTE% is shown in the Figure 3-2 (a - e), where X-axis is logarithm of 10 times controlled open time,  $\log(10 \times T)$ , and the Y-axis is logarithm of 10 times actuator's actual operating open time error percentage,  $\log(10 \times OTE \%)$ .

Figure 3-2 (a - e) shows that for each duty cycle percentage combination, different pressure provided similar tendency, i.e., the longer controlled open time was, the smaller logarithm OTE% value became. Figure 3-2 (a) shows somewhat wider range of logarithm OTE% between each pressure condition when the duty cycle percentage was set to 5%, but the order of each pressure condition at the same controlled open time was random. In contrast to Figure 3-2 (a), Figures 3-2 (b) to (e) show that the ranges of logarithm OTE% values for different pressures were much narrower at the same controlled open time. Therefore, except for the 5% duty cycle percentage condition, which was mostly unstable, the OTE% was independent of operational pressure.



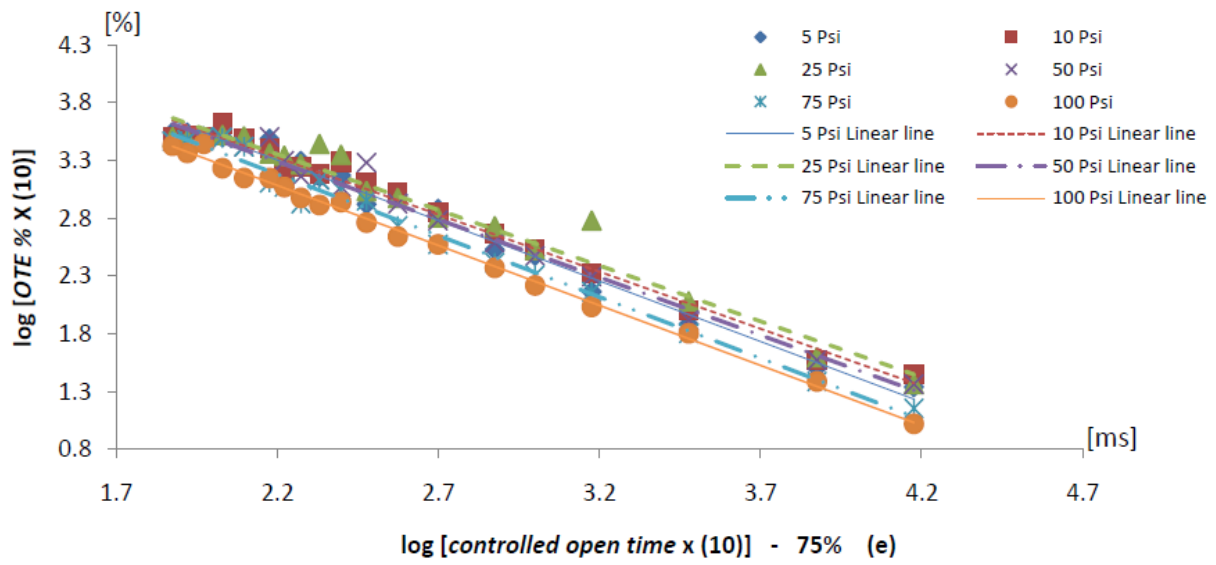
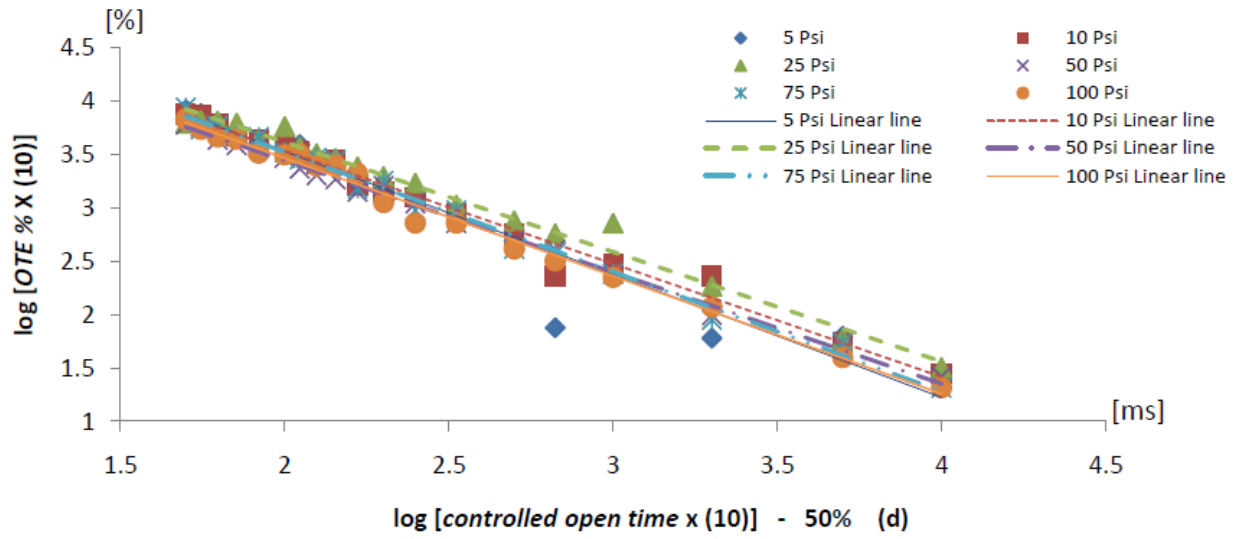
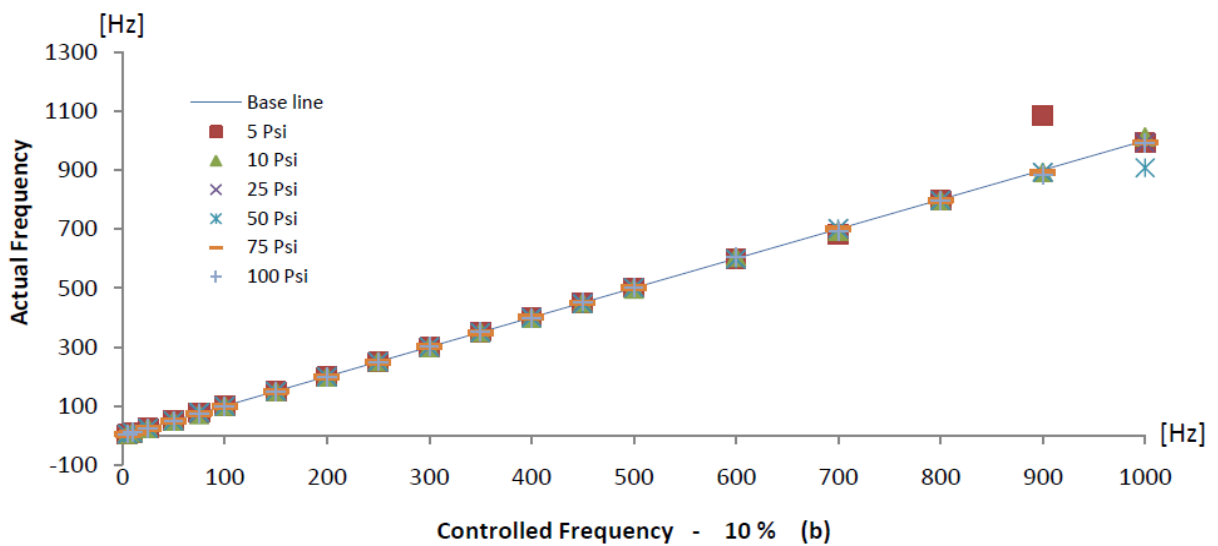
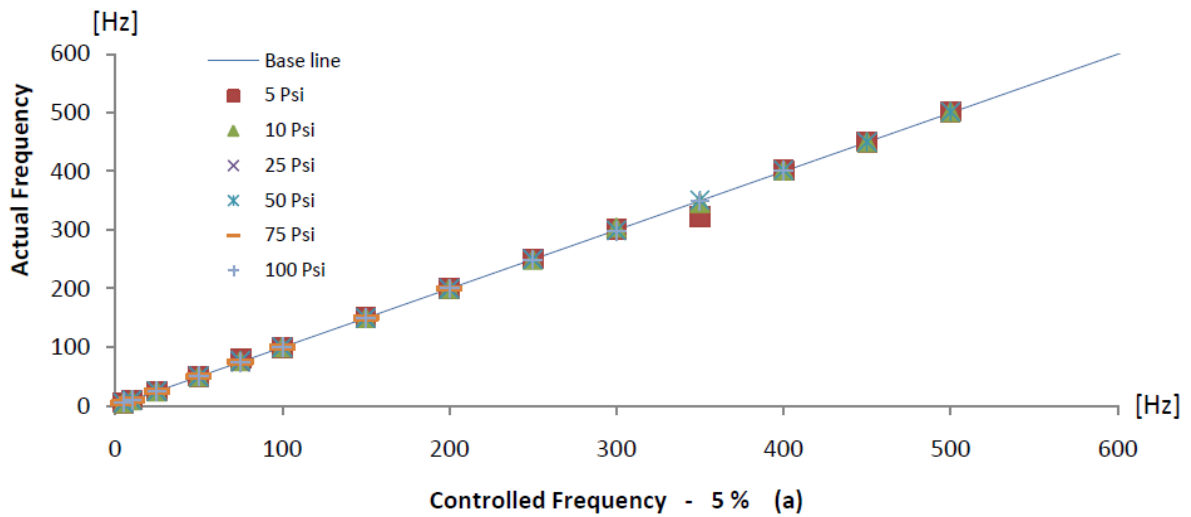


Figure 3-2 pressure dependence for logarithm OTE% at specific logarithm controlled open time

From the above discussions, the actual operating open time of the actuator was not consistent with the controlling signals for open time. Nevertheless, the actuator practical performance of frequency was reliable. As the result shown in Figure 3-3 (a) to (e), the X-axis is the controlled signal for frequency and the Y-axis is the actual operating frequency of the actuator. It is quite straightforward to see that the actual operating frequency for all experiment combinations corresponded to the controlling frequency.



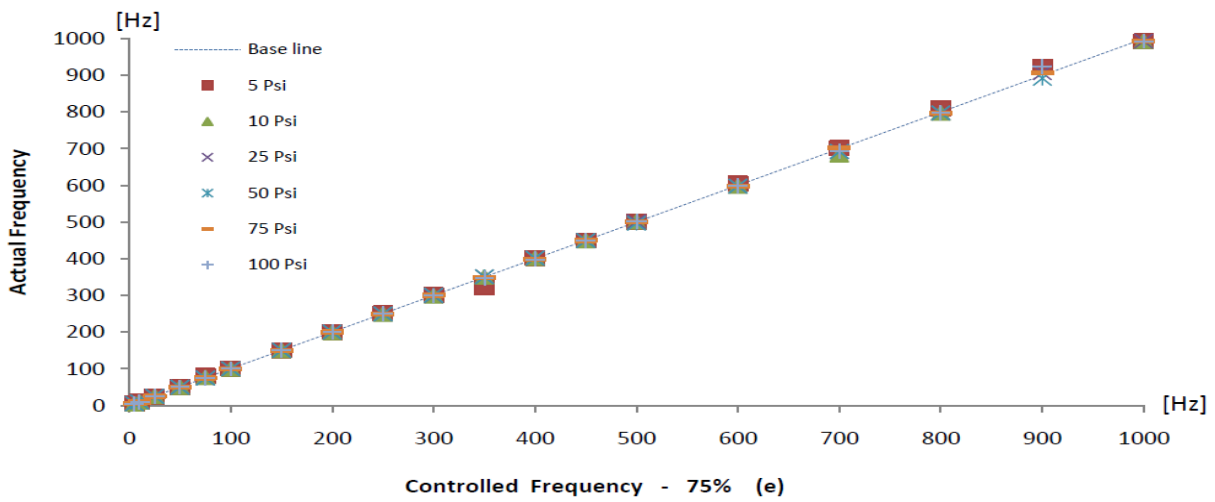
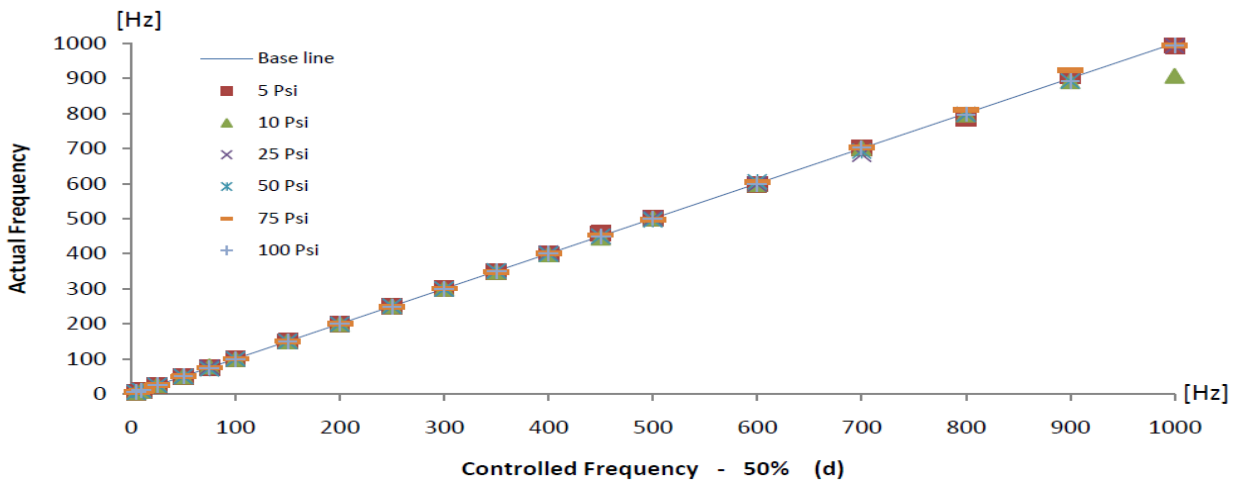
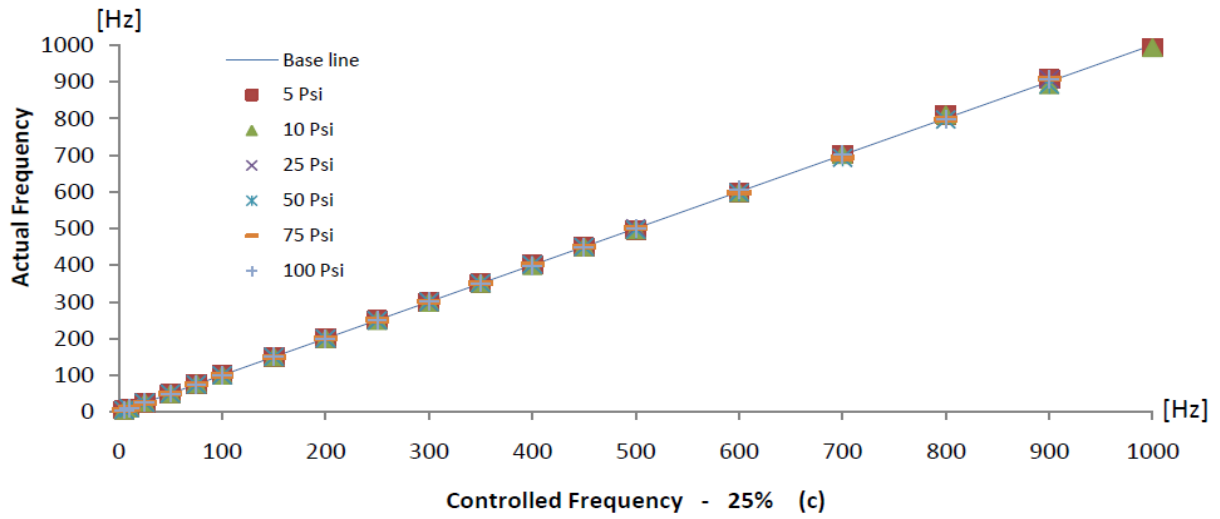


Figure 3-3 actual frequency performance

Under the microscope with the high speed camera observation in this section, the basic characteristic of the actuator had been gained. When the actuator operated under shorter open time, the error of the actual open time increased, but the error was not a function of pressure for the actuator. Although there was error in the actuator's open time, the frequency of the actuator was robust under all condition. The reason is that the actuator's extended open time only occupied the close time in the cycle, so that the performance of the actual frequency corresponded to the controlling signal.

## (2) Jet Issue Into Microchannel (Gas Main Flow)

From previous experiments, the properties of the actuator were obtained. In this experiment, the droplets were introduced into the microchannel in order to assure the actual operating capability of the actuator. The device stage, which connected with the micro device shown in Figure 2-2, was placed right above the microscope and the high speed camera for capturing the images from the microchannel. The droplets of the actuator were introduced into the microchannel via a slit located 4,500  $\mu\text{m}$  downstream the inlet. The slit was 1,200  $\mu\text{m}$  long and 20  $\mu\text{m}$  wide in the stream-wise direction. The main gas flow entered the microchannel at 5 Psi in order to carry droplets out from the observation window.

From the data shown in Figure 3-4 (a) to (f), the X-axis indicates the controlling signal for frequency, and the Y-axis represents the actual operating frequency error percentage (AFE%) of the controlled jets in Equation (3). Moreover, the bar-diagram in each chart expresses the limits of the actual operating frequency of droplets under different conditions of duty cycles in the microchannel.

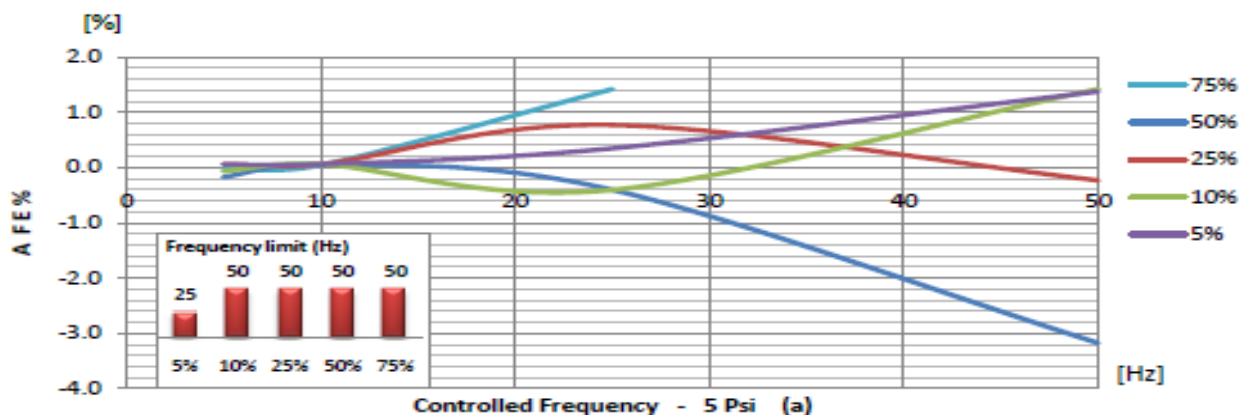
$$[AFE \%] = \left( \frac{R_f - C_f}{C_f} \right) \times 100 \% \quad (3)$$

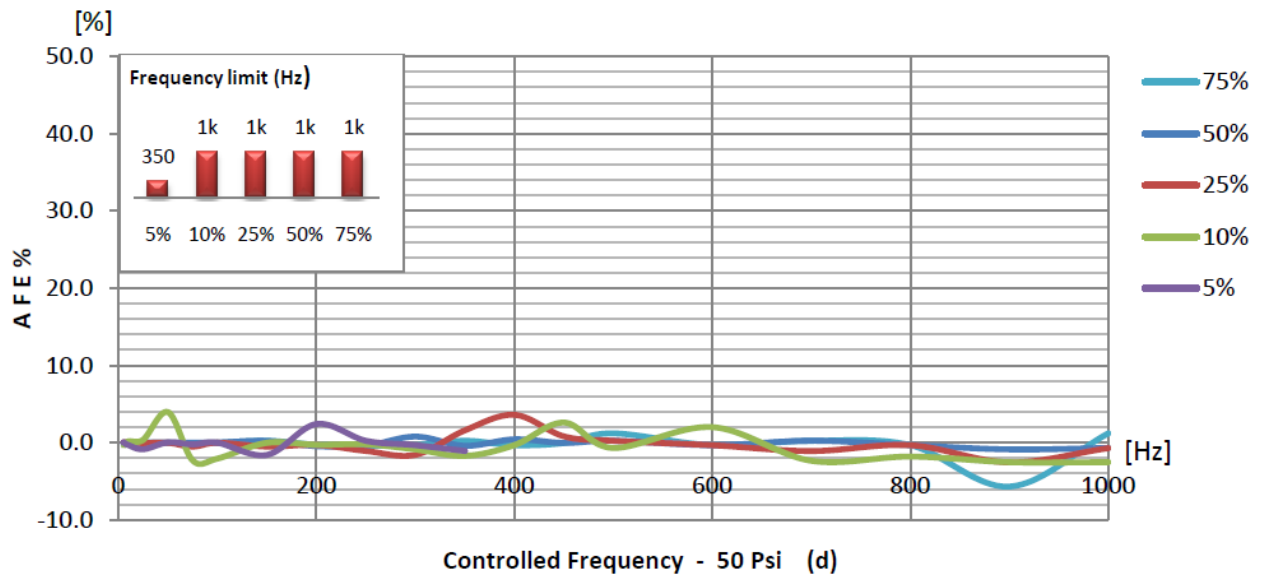
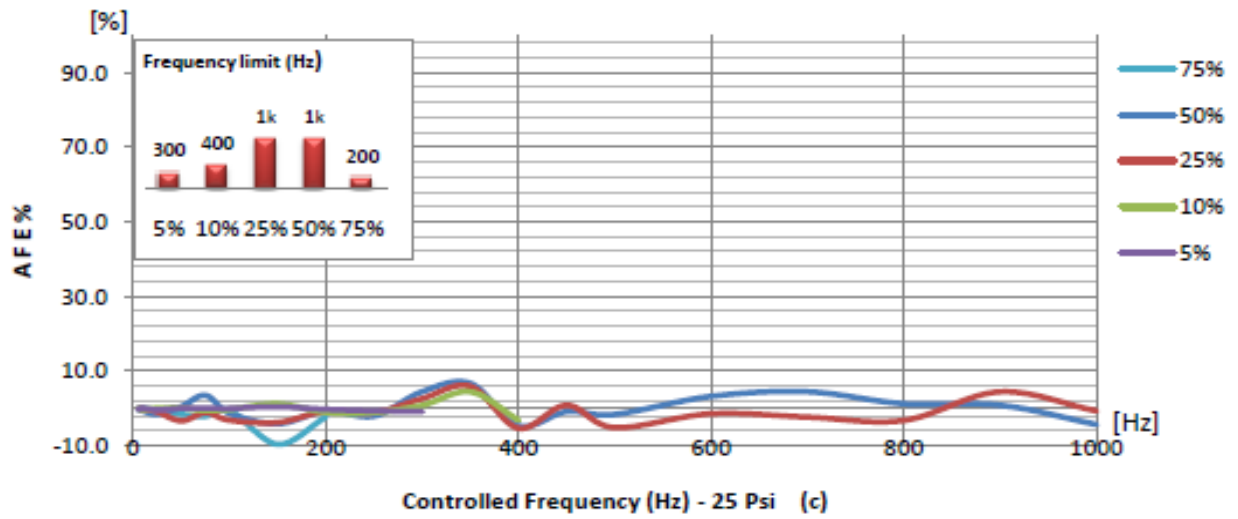
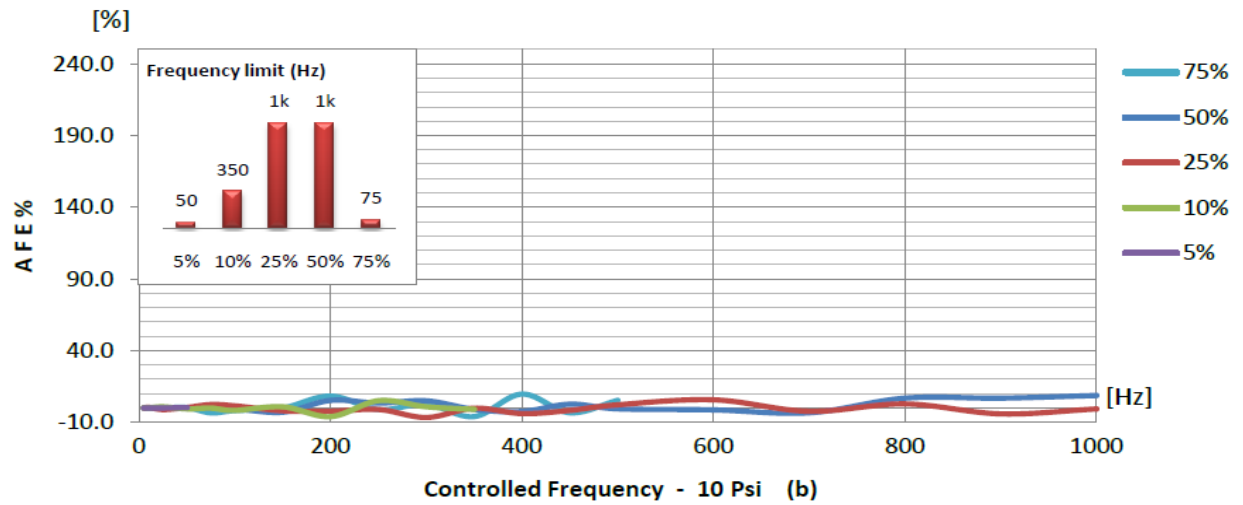
where  $R_f$  is the actual operating frequency of droplets, which obtained from the microscope with the high speed camera observation, and the  $C_f$  is the controlled frequency.

Figure 3-4 (a - f) shows that the ranges of PFE % were all under  $\pm 10\%$  for all pressure. However, the actual operating frequency under the microchannel had its limitation. In Figure 3-4

(a), the bar-diagram shows the highest actual operating frequency allowing up to 50 Hz for a duty cycle percentage of 10%, 25%, 50%, 75%, and the lowest actual operating frequency was only up to 25 Hz for the condition of 5% duty cycle percentage. In this case, when the pressure was 5 Psi and the actuator was operating beyond the highest limit for actual operating frequency in each duty cycle condition, the droplets could not be introduced into the microchannel. Figure 3-4 (b) in which the pressure was 10 Psi shows that each highest actual operating frequency limit was greater than that under 5 Psi. Furthermore, the actual operating frequency limits remained unchanged at 25% and 50% duty cycle percentages and could be operated up to 1000 Hz. However, similar to the 5 Psi condition, the actuator operated over the limit of the highest actual operating frequency for 5% and 10% duty cycle percentage, which resulted in the absence of droplets in the microchannel — the water sheet slowly flowed into the microchannel from the slit without any apparent frequency pulse after the duty cycle percentage reached 75%.

Similarly, for the 25 Psi condition shown in the Figure 3-4 (c), the highest actual operating frequency at 75% duty cycle percentage had slightly risen to 200 Hz, but beyond that, similar to the situation at the same duty cycle under 10 Psi, the water sheet flowed out from the slit into the microchannel continually without any apparent frequency. However, for the duty cycle percentages at 5% and 10%, the frequency could not be examined when the actuator ran over the frequency limit due to the extremely small volume flow rate seeping into microchannel without any frequency. Yet, in cases where the pressure for the actuator was increased, as the results shown in the Figure 3-4 (d), (e), (f), not only all the AFE % were maintained under, but also the highest actual operating frequency for each duty cycle percentage could reach 1000 Hz except for 5% duty cycle for these pressure condition in which the frequency was not detectable.





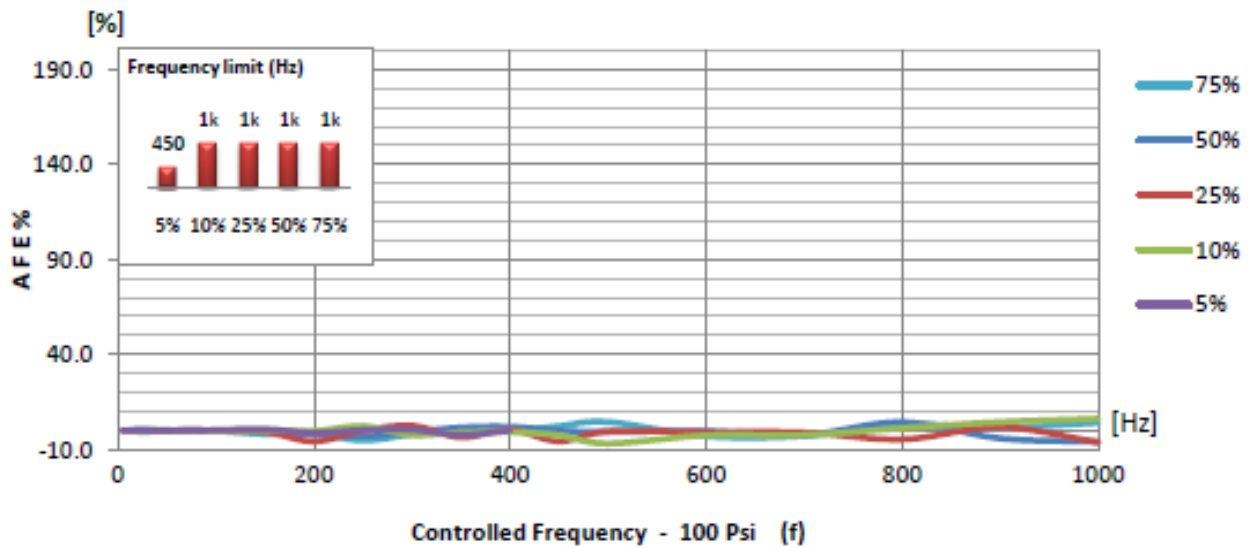
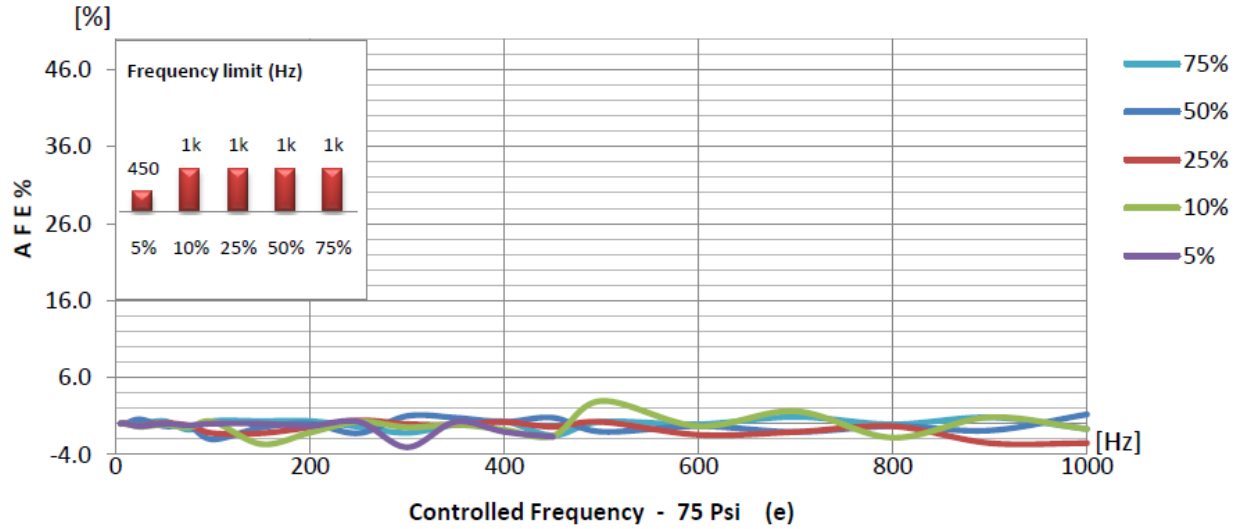
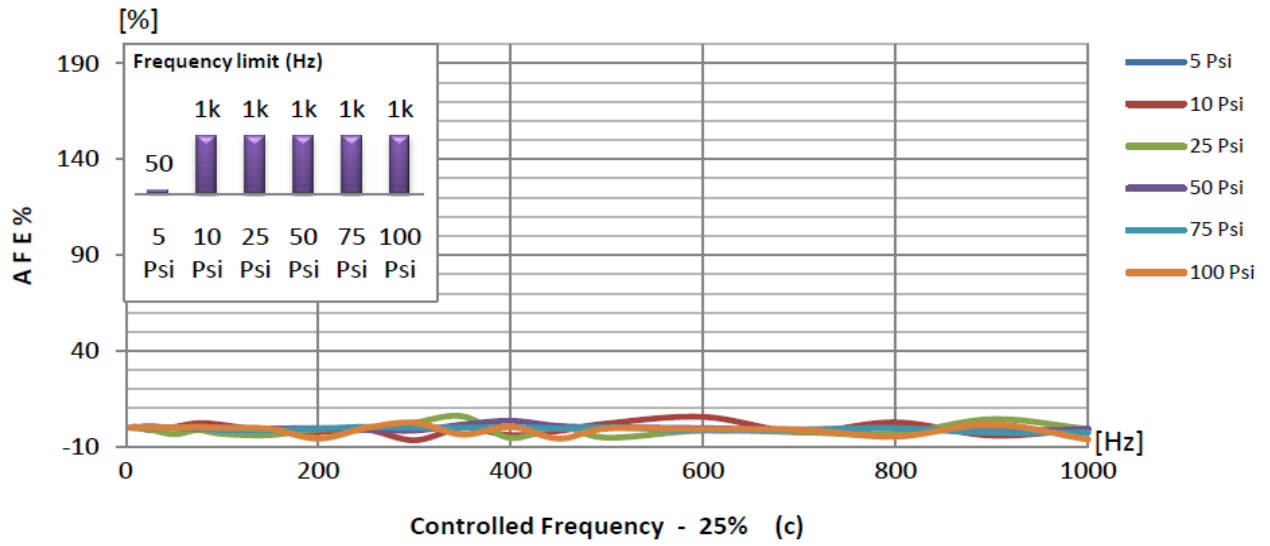
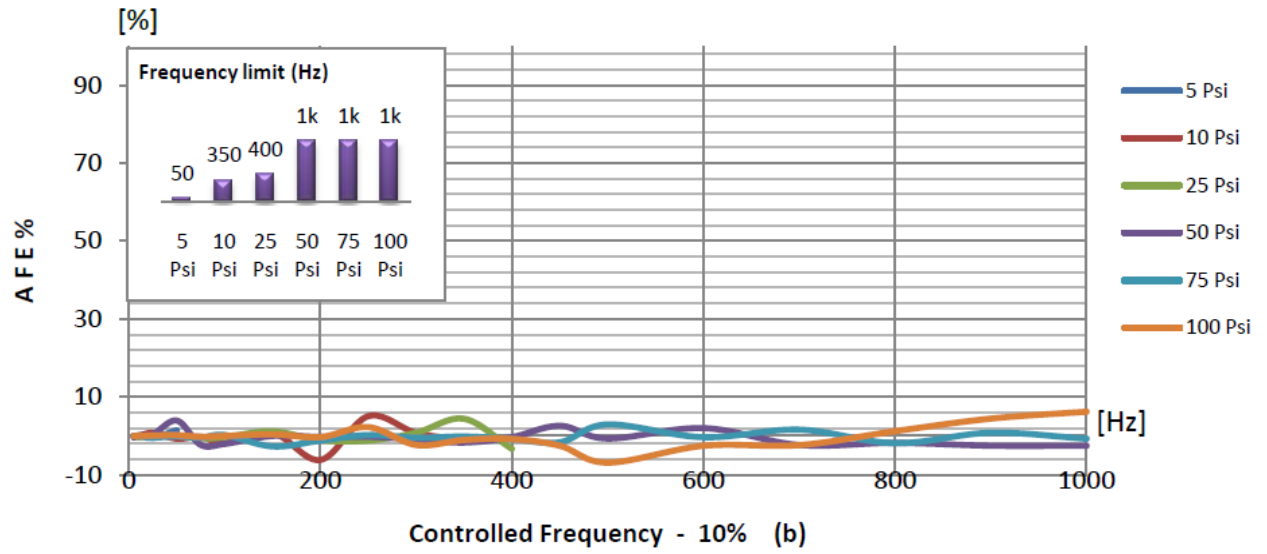
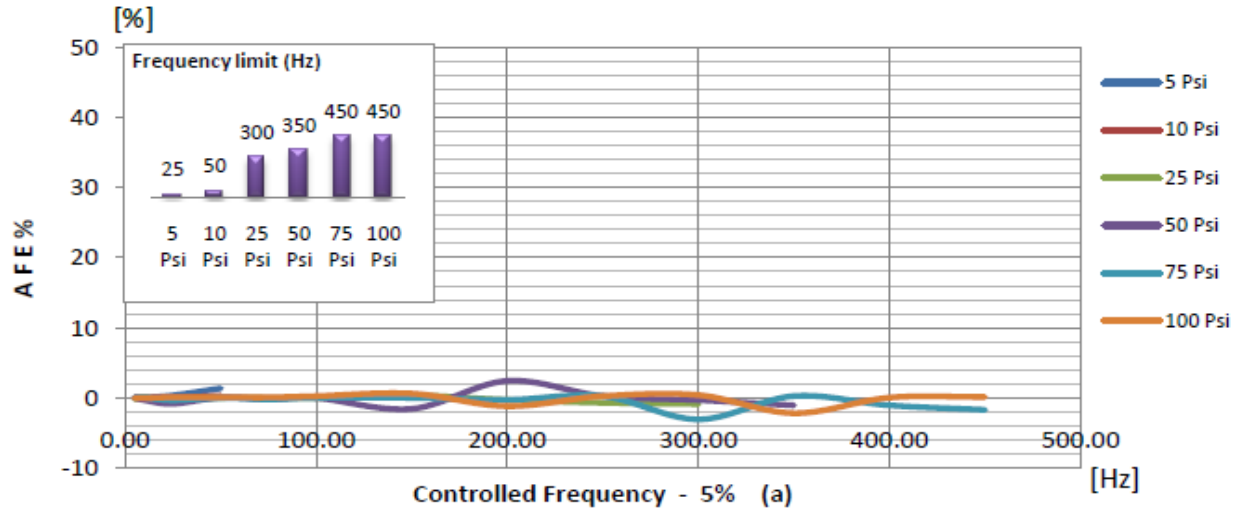


Figure 3-4 AFE % for pressure dependence

Figure 3-5 (a-e) shows the relationship between AFE % and pressure condition. It is clear that when the pressure was increased, the AFE % did not rise for every duty cycle percentage condition. It is also evident that the highest actual operating frequency was increased when the pressure was increased. The same trend was observed for larger duty cycle, i.e., larger duty cycle percentage yielded higher actual operating frequency limit. However, when the duty cycle increased to 75%, the same result of exceeding actual operating frequency limit in 5 Psi, 10 Psi and 25 Psi occurred — water sheet flowed out from the slit continuously without pulsating.



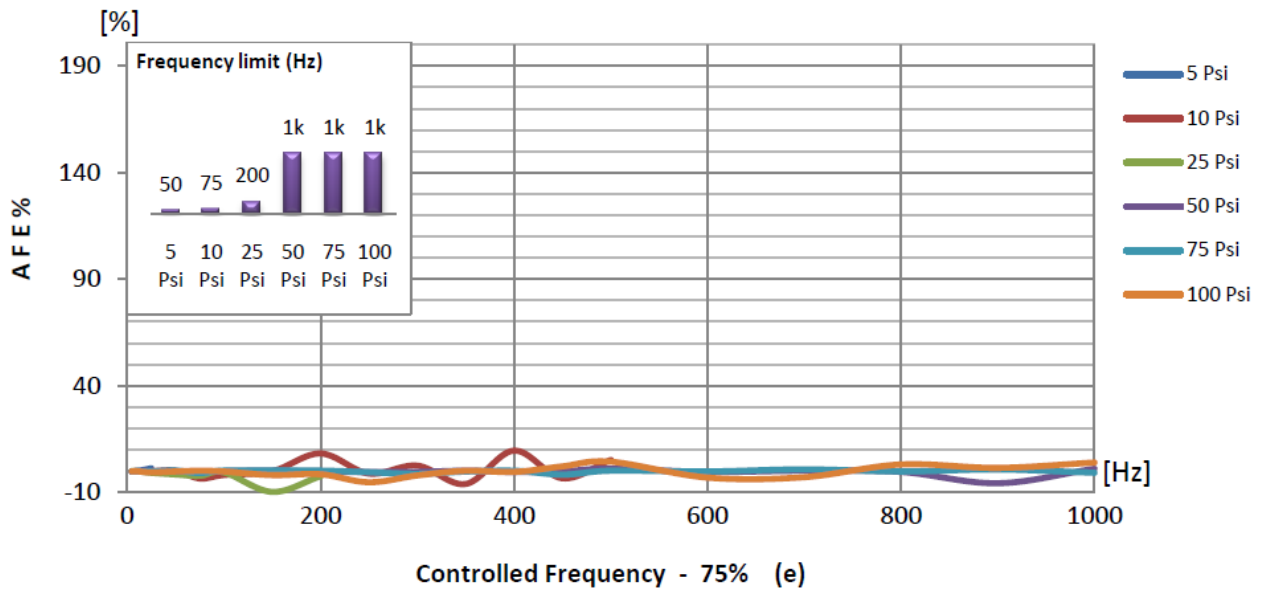
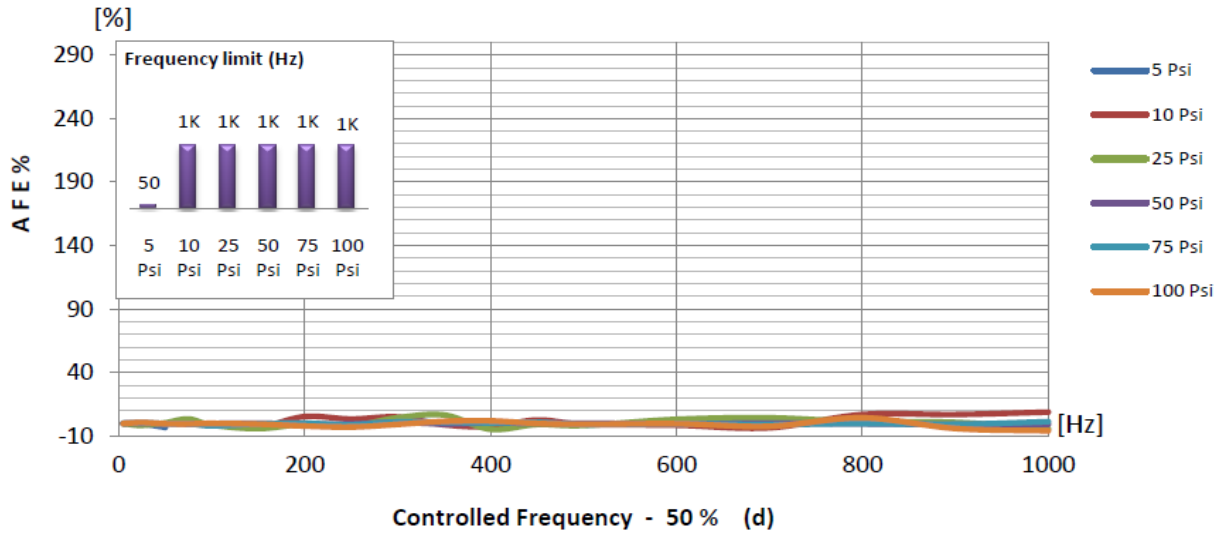


Figure 3- 5 AFE% for duty cycle dependence

Generally, the experimental data in this section suggest that both lower pressure and lower duty cycle percentage could limit the actual operating frequency of the valves below 1000 Hz. Beyond the highest limit of actual operating frequency, the flow issued from the slit without apparent frequency. The cause for this phenomenon was the fluidic vias between the device stage and the micro device. Figure 3-6 is a schematic drawing of the cross section for the connecting zone between the actuator nozzle and the micro device. As the diagram shows, the gap between the micro device and nozzle formed a chamber in the stage. However, the chamber could modify the fluidic frequency and magnitude of the droplets, so the droplets passing through the slit were

affected. When the actuator operated at low pressure with low duty cycle percentage and operated with higher frequency, the size of each droplet was much smaller. Therefore, the small volume of the droplets did not have enough kinetic energy to pass through the slit on the micro device due to the large pressure drop, caused by the large dimension difference between the slit and the chamber space. After the droplets filled the chamber, the liquid started to flow slowly into the microchannel.

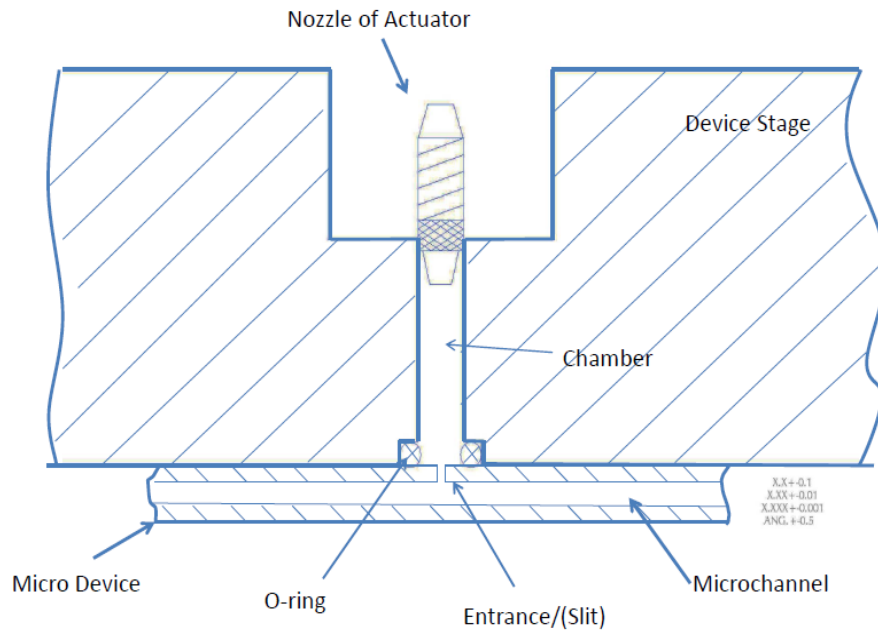


Figure 3- 6 cross-section schematic diagram for the connecting zone

When the duty cycle percentage was high (75% in this experiment), which implied longer actual operating open time of the actuator, high volume flow rate was issued into the chamber. As a result, considering the lower pressure conditions such as 5 Psi, 10 Psi and 25 Psi, the droplets were introduced into the chamber before the previous droplets departed from the chamber into the microchannel. Consequently, it caused the droplets to coalesce in the chamber forming a water sheet that flowed into the microchannel continuously. In order to improve the control robustness of the droplets/disturbances in the microchannel, the design of the connection between the stage and micro device should be modified.

Additionally, the magnitude of jet in the microchannel was related to pressure of the liquid reservoir, which was a critical variable for the volume flow rate. The pictures shown in Figure 3-7 were taken under the microscope and high speed camera with a frame rate of 2100 per second and interval frame time of 476 microseconds. The images on the columns of Figure 3-7 show the droplet entering into the microchannel from the slit. From Figure 3-7 (b) and (c), it can be seen that the droplet came out from the slit slowly and smoothly. Furthermore, the droplet remained laminar. As the pictures, shown in Figure 3-7, with increase of the pressure in the liquid reservoir of the actuator, the velocity increased as well. When the droplets were pressurized to a higher value, (Figure 3-7 (e) and (f)), the water sheets moved farther.

However, the actuator's main characteristic was introduced, but it depended on the conditions of the working environment, such as the shape and dimension of the slit or orifice, which the droplets come out from. All of these were the variables that affected the volume flow rate of the jet. Therefore, for more precise data, applying  $\mu$ PIV technique to measure velocity was needed.

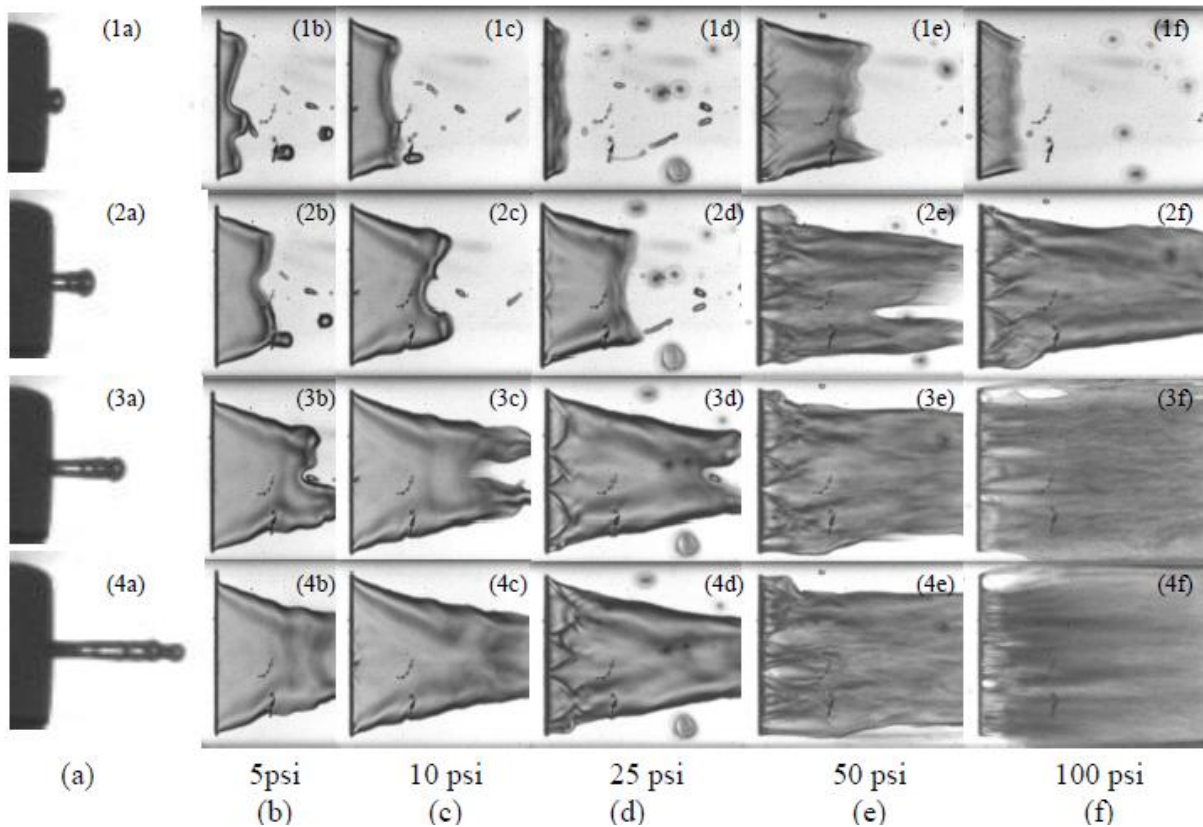


Figure 3-7 Illustration for the droplets in microchannel

## IV. CONCLUSION

In this thesis, the basic characteristics and the reliability of a flow control device for micro fluidic applications has been examined. The actuator parameters, i.e., frequency, duty cycle percentage, and pressure, have also been quantified and presented. The following is the summary of the actuator's properties and the relationships between the parameters.

- For the basic characteristic of the actuator, shorter controlled open time, which depended on the controlled duty cycle percentage and frequency, held larger value of OTE %.
- Despite the presence of OTE%, the performance of actual operating frequency of this actuator was robust and corresponded to the controlled value. The reason was that the actuator open time occupied the close time in the cycle, but it did not affect the open timing of the subsequent cycle.
- The OTE% was independent of the working pressure condition.
- When the droplets were introduced into microchannel, the range of the AFE% of the droplets was  $\pm 10\%$ , which was sufficient for providing robust frequency in the microchannel.
- However, there were some limitations on the actual operating frequency with the microchannel. For lower pressure, such as 5 Psi, actual operating frequency of the droplets in the microchannel was allowed only up to 50 Hz ~ 75 Hz for each duty cycle percentage.
- Under pressures above 25 Psi, the actual working frequency, which allowed the actuator to operate up to 1000 Hz, could only be achieved for 25% and 50% duty cycle percentage conditions.
- The limit of highest actual operating frequency could be augmented while the working pressure was increased. Yet, under every pressure condition examined in this experiment, the performances of the actual operating frequency in microchannel for 5% duty cycle percentage had deficiency — the highest limit for actual operating frequency was allowed only up to 450 Hz in the 75 Psi and 100 Psi pressure conditions.

Using micro-dispensing valve for flow control actuator in order to create disturbances in microchannel is a new concept and technique in the research field of micro-scale heat transfer. Owing to the issue of connecting parts between nozzle and the micro-device in this experiment,

there is a drawback for the performance in actual frequency responding in the microchannel. Moreover, the different types of micro devices possess the diversity in the flow control entrance sizes on the micro device surface. The relative small entrance dimension compared to the chamber between nozzle and the micro device allows serious pressure drop to occur, and to affect the actual operating performance of the droplets in the microchannel. To address this issue, the working pressure in the liquid reservoir for flow control system should be greater than 25 Psi so as to withstand the pressure drop. Additionally, the volume flow rate of the droplets in the microchannel can be obtained by the product of droplets velocity, which can be measured by  $\mu$ PIV technique and the dimension of the slit/orifice in the microchannel.

## REFERENCES

- [1] Kosar, A. Mishra, C., and Peles, Y. "Laminar Flow Across a Bank of Low Aspect Ratio Micro Pin Fins." *J. Fluids Engineering* 127 (2005) 419.
- [2] W. Owhaib, B. Palm, "Experimental investigation of single-phase convective heat transfer in circular microchannels." *J. Experimental Thermal and Fluid Science* 28 (2004) 105.
- [3] P. Lee, S. Garimella, Investigation of heat transfer in rectangular microchannels, *Int. J. Heat Mass Transfer* 48 (2005) 1688.
- [4] G. Celata, M. Cumo, G. Zummo, "Thermal-hydraulic characteristics of single-phase flow in capillary pipes." *J. Experimental Thermal and Fluid Science* 28 (2004) 87.
- [5] J. Li, G. Peterson, P. Cheng, "Three-dimensional analysis of heat transfer in a micro-heat sink with single-phase flow." *Int. J. Heat Mass Transfer* 47 (2004) 4215.
- [6] S. Kandlikar, W. Grande, "Evaluation of single-phase flow in microchannels for high heat flux chip cooling-thermohydraulic performance enhancement and fabrication technology." *Int. J. Heat Transfer Engineering* 25 (2004)
- [7] A. Kos\_ar, C.J. Kuo, Y. Peles, Boiling heat transfer in rectangular microchannels with reentrant cavities, *Int. J. Heat Mass Transfer* 48 (2005) 4867.
- [8] S.G. Kandlikar, Two-phase flow patterns, pressure drop, and heat transfer during boiling in minichannels flow passages of compact evaporators, *J. Heat Transfer Eng.* 23 (1) (2002) 5.
- [9] W. Qu, I. Mudawar, Flow boiling heat transfer in two-phase microchannel heat sink: Part 1. Experimental investigation and assessment of correlation methods. *Int. J. Heat Mass Transfer* 46 (2003) 2755.

[10] Haecheon Choi, Woo-Pyung Jeon, and Jinsung Kim. "Control of Flow Over a Bluff Body." *Annu. Rev. Fluid Mech.* 2008.40:113-139

[11] Clarence W. Rowley and David R. Williams. "Dynamics and Control of High-Reynolds-Number Flow over Open Cavities." *Annu. Rev. Fluid Mech.* 2006.38:251-276

[12] S.D. Hwang, C.H. Lee, H.H. Cho. "Heat Transfer and Flow structure in axisymmetric impinging jet controlled by vortex pairing" . *Int. J. of Heat and Fluid Flow* 22 (2001) 293

[13] Kyoji Inaoka, Kazuya Nakamura, Mamoru Senda. "Heat Transfer Control Of Backward-Facing Step Flow In A Duct By Means Of Miniature Electromagnetic Actuator" *Int. J. of Heat and Fluid Flow* 25 (2004) 711

[14] Gad-el-Hak, M., *Flow Control: Passive, Active and Reactive Flow Management*, Cambridge University Press, London, United Kingdom 2000.